

Non-linear Behavior Assessment and Fatigue Analysis of Ankle Foot Orthosis by Finite Element Method

Thien Tich Truong^{1,2,*}, Khuong Trieu Nguyen^{1,2}



Use your smartphone to scan this QR code and download this article

¹Department of Engineering Mechanics, Faculty of Applied Sciences, Ho Chi Minh City University of Technology, 268 Ly Thuong Kiet Street, District 10, Ho Chi Minh City, Vietnam.

²Vietnam National University Ho Chi Minh City, Linh Trung Ward, Thu Duc District, Ho Chi Minh City, Vietnam.

Correspondence

Thien Tich Truong, Department of Engineering Mechanics, Faculty of Applied Sciences, Ho Chi Minh City University of Technology, 268 Ly Thuong Kiet Street, District 10, Ho Chi Minh City, Vietnam.

Vietnam National University Ho Chi Minh City, Linh Trung Ward, Thu Duc District, Ho Chi Minh City, Vietnam.

Email: ttruong@hcmut.edu.vn

History

- Received: 2021-09-06
- Accepted: 2021-11-21
- Published: 2022-02-11

DOI : 10.32508/stdj.v24iS11.3818



Copyright

© VNUHCM Press. This is an open-access article distributed under the terms of the Creative Commons Attribution 4.0 International license.



ABSTRACT

Thanks to the rapid development of orthopedic technology, many types of orthopedics have been created to help patients with disabilities. Orthopedic ankle-foot surgery (AFO) is one of the most common prescriptions for orthopedic lower extremities. In the past, there have been some experimental studies but not fully addressed analytically. This study begins with the modeling and prediction of the non-linear behavior of AFOs non-joint plastic. Large strain effects and non-linear materials are included in the formulation and their influence on results assessed. AFO has two important factors: rotational stiffness and fatigue life, which have not been widely studied. In this study, the Newton-Raphson method is used to investigate the non-linear behavior of plastic ankle insoles (AFOs) through finite element modeling; the results are compared with the reference study to clarify. Since then, the finite element method will be applied to all models to determine the relationship between AFO trimline position and rotational stiffness for moderate and large rotation in plantar flexion and dorsiflexion. The results of stiffness rotation suggested that stiffness analysis of the orthotropic is effective as the help for the doctor in prescribing patients. In the fatigue analysis, the structure is assumed that used in the range of repetitive loads, the S-N curve of the Polypropylene material was used to the definition of material. The number of steps is investigated to define the life cycles of the orthotropic through the variation thickness to find the optimum thickness to meet the fatigue strength. Through careful consideration and specification of key modeling parameters, the finite element method is a reliable and efficient alternative for analyzing the non-linear behavior and fatigue life of AFO designs, as simulation and empirical results are nearly possible.

Key words: Ankle foot orthosis, orthosis stiffness, orthosis trimline, plantar flexion, fatigue

INTRODUCTION

AN ankle-foot orthopedic device (AFO) is a widely used orthopedic device for patients with various muscles and joint weakness and instability in the lower extremities¹. The range requirements for AFO bidirectional flexion resistance vary according to the medical state, for example, for patients with stroke², muscular diseases³, or for diseases are children⁴. Over the last 30 years, AFO research has been conducted to investigate the stiffness qualities of standard AFO designs⁵⁻⁷. The use of computers facilitates the design of AFOs with advantages such as design flexibility, production speed, quality consistency, and standardization⁸. Darwich⁹ evaluated two methods to the AFO problem, one traditional and one utilizing computer tools, and the findings revealed that the use of computer tools had more advantages. Combining simulation with experimentation in computer-aided bioengineering gives the benefit of freedom in choosing shape and materials, but it needs values to be anticipated in the process; the simulation must be established consistently. The model considered in this

study is described in Figure 1. Several evaluations of plastic AFOs were carried out using the tried and true finite element method (FEM)¹⁰⁻¹². Various designs of AFO have also been evaluated by Surmen¹³ based on FEM.

Most of the previous reviews have assumed that the behavior of the structure is linear. This implies that large strains and non-linear material effects are ignored. When the load range of polypropylene exceeds a certain point, however, it becomes a non-linear material. Polypropylene materials have advantages, such as durability and a shown ability to construct orthopedic devices better than metal rods¹. Still, it is difficult to anticipate their mechanical behavior under real-world settings¹⁴. Experiments^{6,7,14} provide clear evidence for the AFO's geometric and physically non-linear behavior.

This research focuses on constructing an AFO model and analyzing the non-linear behavior of materials with a large deformation effect under static load. FEM analysis is first performed on a single model, a 40 percent trimline AFO design, to assess the impact of geometrical and material nonlinearities. This is

Cite this article : Truong T T, Nguyen K T. **Non-linear Behavior Assessment and Fatigue Analysis of Ankle Foot Orthosis by Finite Element Method.** *Sci. Tech. Dev. J.*; 24(S11):SI25-SI31.

followed by systematic simulation of AFO samples with variable cutouts to predict AFO stiffness. And finally, AFO is analyzed in terms of fatigue to find out an optimization thickness. Finite element analysis was performed on ANSYS software, academic version 2021R1.



Figure 1: AFO Model

BASIC OF THEORIES

Non-linear Static Analysis

In the finite element method, the applied load on the system is approximated by a system of forces placed at the nodes of the element (external force). Similarly, the stress components of the system can be replaced by a system of forces located at the nodes of the element (internal force). According to the principle of balance, these two force systems must be equal. However, in the iteration steps of the non-linear analysis problem, the difference between these two force systems always exists and decreases as the number of iterations increases. When this difference is less than a specified value, the problem converges. In the problem of non-linear materials, the Newton-Raphson iterative method is employed. It approximates non-linear problems to linear problems by breaking down the load into increasing load steps. The stiffness matrix K will be re-generated after each load step because of the change in stiffness due to the effect of the strain. This iterative process can be briefly described as equation (1)¹⁵:

$$K(q_i)q_i = F(q_i) \quad (1)$$

where: $K(q_i)$: tangent stiffness matrix of load step i
 q_i : deformation of load step i
 $F(q_i)$: force of load step i

Fatigue Analysis

Fatigue Analysis is the structural analysis of the failure tendency of systems when they are subjected to cyclical loads. Fatigue is the progressive and localized structural damage that happens when a test model is subjected to cyclic loading. Continued cycling of high-stress concentrations may eventually cause a crack that propagates and leads to failure.

In this study, fatigue analysis is performed by using the Stress-Life (S-N) or S-N method. An S-N curve usually characterizes materials fatigue performance, also referred as a Wöhler curve. This is often plotted with the cyclic stress (S) against the cycles to failure (N) on a logarithmic scale. S-N curves are derived from tests on samples of the test model to be characterized (often called coupons or specimens). Daily sinusoidal stress is applied by a testing machine, counts the number of cycles to failure. In the presence of gentle stress superimposed on the cyclic loading, the Goodman relation (Equation (2)) is often utilized to estimate a failure condition. It plots stress amplitude against mean stress with the fatigue limit and the material's ultimate tensile strength as the two extremes. Alternative failure criteria include Gerber and Soderberg are described in Figure 2.¹⁶

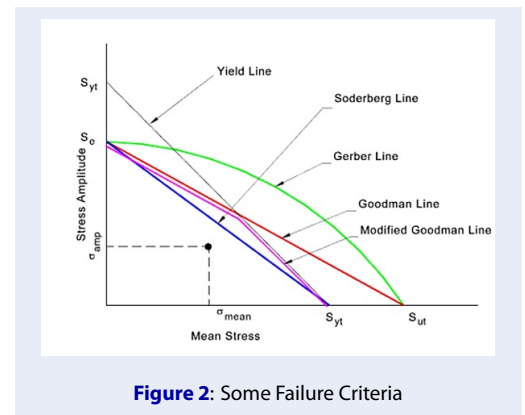


Figure 2: Some Failure Criteria

Goodman criteria:

$$\frac{1}{n} = \frac{\sigma_a}{S_e} + \frac{\sigma_m}{S_{ut}} \quad (2)$$

Where:

n : safety of factor

σ_a : mangnitude stress

σ_m : mean stress

S_e : fatigue limit

S_{ut} : ultimate tensile strength

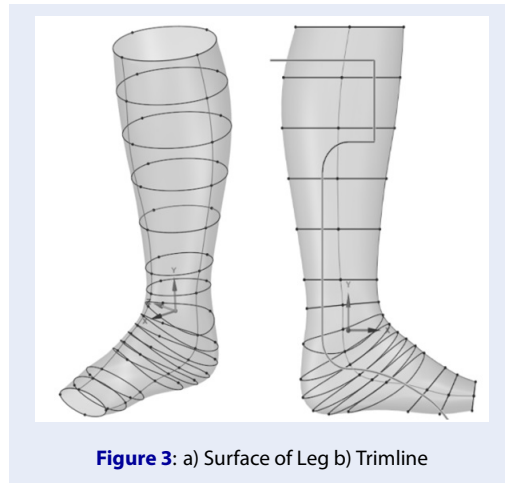


Figure 3: a) Surface of Leg b) Trimline

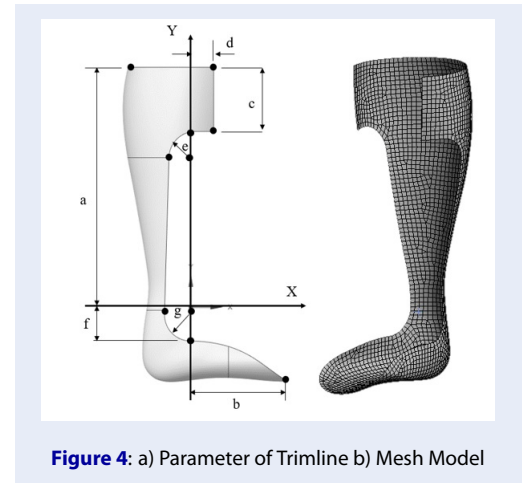


Figure 4: a) Parameter of Trimline b) Mesh Model

SIMULATION

Model

The coordinates of several points located on the surface of a normal human right lower limb are measured from the drawings of the lateral and anterior profiles of the limb as well as the cross-section of the foot. These points are distributed around the circumference of several cross-sections through the calf to the foot⁵. The surface area of the leg is constructed by using the surface tool that passes through closed curves of the sections, as shown in Figure 3a.

The trimline is combined from straight segments and arcs in the two-dimensional plane of the leg as shown in Figure 3b. A set of parameters has been chosen to determine the position of the points. Accepted values for trimline in this study are $a = 260$ mm, $b = 110$ mm, $c = 80$ mm, $d = e = f = g = 30$ mm (Figure 4a)³. The distance from the heel to the origin in the vertical direction is 83 mm, and in the horizontal direction is 55 mm. The cutting surface is created by extending the cut line in the z -direction. The model is divided into smaller areas that facilitate the imposition of applied loads and boundary constraints.

Shell181 element is selected in this paper to model AFO. The displacement and stress results converge with the mesh level, including 2792 nodes and 2705 elements. It is assumed that the AFO has a constant thickness of 2 mm throughout the analysis. Figure 4b shows the model after meshing.

Material

In this study, Polypropylene (PP) material was chosen because it is used mostly for AFO orthopedic materials and has outstanding properties regarding high mechanical strength, non-toxicity in contact with skin.

The Poisson coefficient of the selected material is 0.35⁵. The stress-strain curve is referenced from the article⁵ with the elastic modulus E of 1390 MPa (Figure 5).

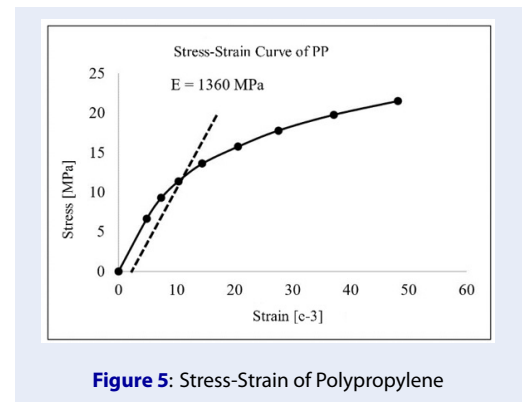


Figure 5: Stress-Strain of Polypropylene

Boundary Condition and Load

One constraint is applied to the calf region to limit radially displacement caused by the calf strap. A cylindrical coordinate system is created with the z -axis coincident with the direction of the tibia, the y -radial direction is the calf circumference, and the x -radial direction is the direction centered on the z -axis. The AFO is therefore only allowed to both rotary and slide up or down the z -axis. Next, constraints are applied on the heel region representing a foot-AFO-heel interaction, for , the tightness between shoe the AFO and the biomechanical properties that consider the heel to rotate around the ankle walk. Therefore, these nodes are constrained in the radial direction by a cylindrical coordinate system with the origin at the ankle center (Figure 6). The lateral and medial is also

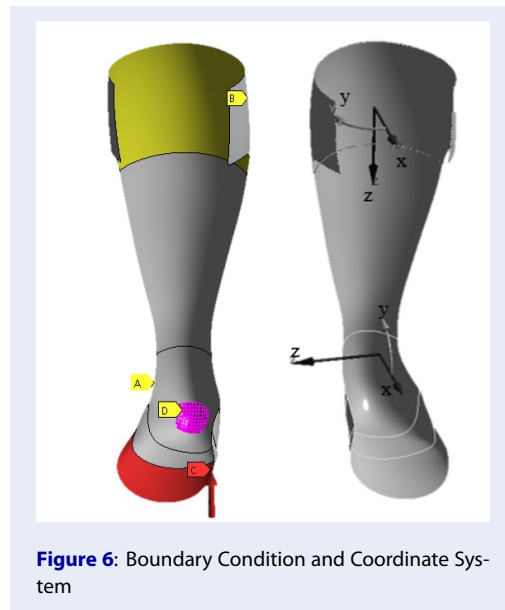


Figure 6: Boundary Condition and Coordinate System

assumed not to move to the sides (the z-direction of the heel cylinder coordinate system), which is thought to be caused by the compression of the shoe; hence, it is also avoids buckling of the plate that significantly affects the rotational stiffness of the structure during dorsiflexion or plantar flexion. A pressure of 8.65 kPa is applied to the area at the distal foot of the AFO for dorsiflexion and plantar flexion. This value is derived from the average force exerted on rotation during a gait cycle¹⁷.

Results of Static Analysis

The results of stress, displacement, and rotation are presented in Table 1. The stress concentration area is the inner surface of the ankle region. The maximum stress value of the analytical is 16.8 MPa which is larger than the yield point (12MPa), so it will cause residual strain after unloading, but this value has not yet exceeded the tensile strength value of PP is 35 MPa¹⁸. It can be seen that without the large deformation effect, both stress and displacement results are the same for both directions; when considering the large deformation, the resulting stress is about 6.5% larger in the plantar flexion, and there is not much change in dorsiflexion with large deformation. This difference results from the changing of stiffness during large deformation. The stress results are also compared with the article, and there is not much discrepancy; the errors are less than 5%. The convergence of the von-Mises stress results is presented in Figure 10. The program automatically adjusts the mesh after each loop, the convergence condition and the maximum number

of solutions are set as the error between two consecutive results is 1% or after 10 solutions that the results do not convergence, then the program will stop solving. The initial mesh level is selected to be 13mm with 766 nodes and 760 elements, after 7 iterations, the error between two consecutive iterations is 0.555% less than 1%, so it meets the convergence condition and has the same number of nodes and elements are 45858 and 45578 respectively.

A series of AFOs models were generated by varying the fillet angle at the ankle (dimension g in Figure 3c). The ratio of the trimline arc radius at the lateral malleolus height is defined as the trimline shape parameter. Apply a displacement to a node at the distal foot of the AFO in the y-direction (Figure 8) so that rotations of 5° and 15° are produced, the constraints are preserved except for the z constraint of the lateral and medial which is removed to resemble the experiment¹⁹. The reaction force generated by the displacement application on the node are used to calculate the bending moment. This moment is the result of the reaction force times the arm R (Figure 8). Figure 9 shows the bending moment of two rotation angles corresponding to dorsiflexion and plantar flexion. It can be seen that for a rotation of 5° the error is up to 63% for 60% of the trimline, and for 15° it is 88% and also for 60% of the trimline. It is assumed that when the percentage of trimline is large than 50% and 60%, the AFO has almost no resistance to bending so it is very sensitive (soft rotation effect) to the applied forces, and this making accurate hardness prediction very difficult^{5,15}. If 50% and 60% trimline are not a consideration, the maximum of the discrepancy are 13% and 26% respectively for 5° and 15° rotation.

Fatigue Analysis

This analysis assumes that a fully reversed load is created in the two-direction stepping process of the AFO (dorsiflexion and plantar flexion), and thus a stress cycle including the compressive stress dorsiflexion and the tensile stress of plantar flexion is generated. The difference between tensile and compressive strength is ignored for the appropriate simplification. The boundary conditions are applied the same as in section 3.3; the pressure value applied to the AFO is 11.2 kPa; this value is averaged from the experiment¹³, the mesh is 5 mm. The AFO sample used has a 40% trimline, 3 AFO samples with thicknesses of 2, 3, 4 mm, respectively. The S-N fatigue curve of polypropylene is showed in Figure 11²⁰. The results are show in Table 2.

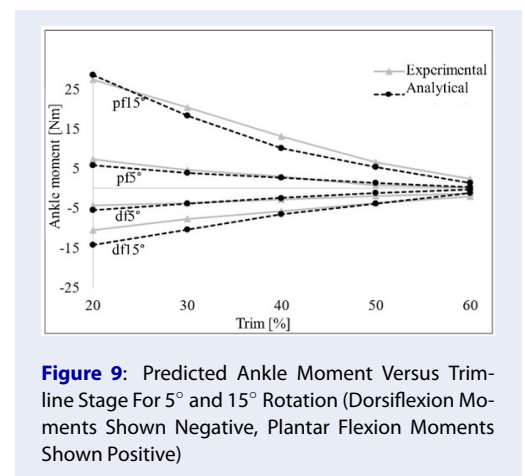
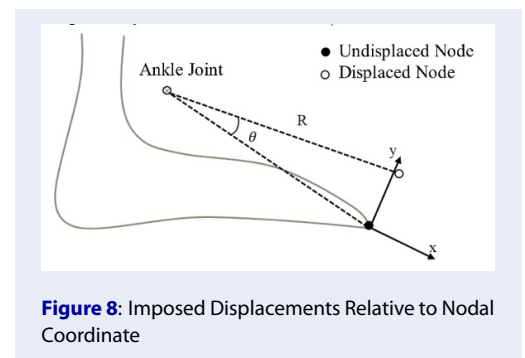
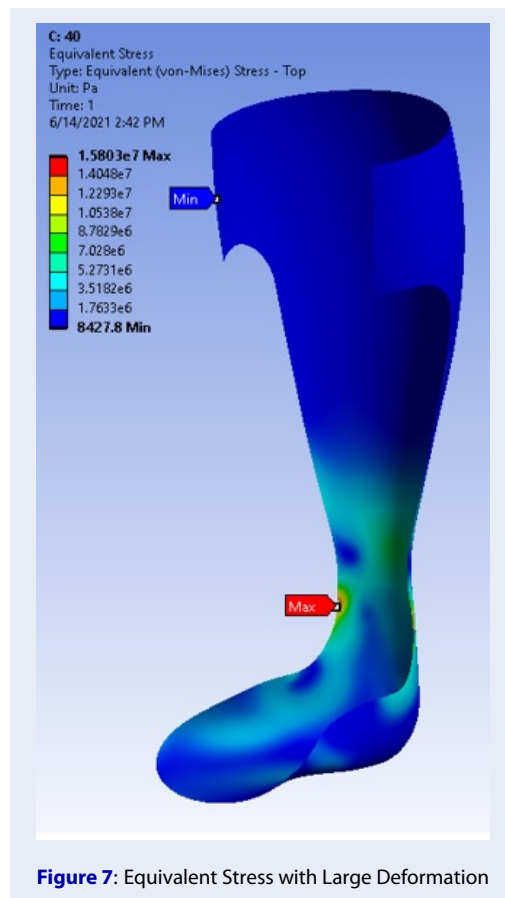
The area of failure distributes in the same area of concentrate stress in Figure 7. The results from Table 7

Table 1: The results of simulation and compare with a 40 percent trimline

Type of analysis	Direction of far foot rotation	Maximum von-Mises stress (top-inner)	Reference paper ⁵	This study	Discrepancy (%)	Maximum deformation (mm)	Rotation angle (degree)
Non-linear (without large deformation)	Dorsiflexion	15,8	15,78	0,12%	12,21	5,1	
	Plantar flexion	15,8	15,78	0,12%	12,21	5,1	
Non-linear (large deformation)	Dorsiflexion	16,2	16,8	3,7%	13,56	8,34	
	Plantar flexion	15,1	15,8	4,6%	11,75	4,89	

Table 2: Life and safety factor of 40% trimline

Thickness (mm)	Cycles (231500steps/300day) ²⁰	Safety factor
2	6619 (8 days)	0,59
3	524850 (2 years 3 months)	0,92
4	> 1 x 10 ⁷ cycles	1,26



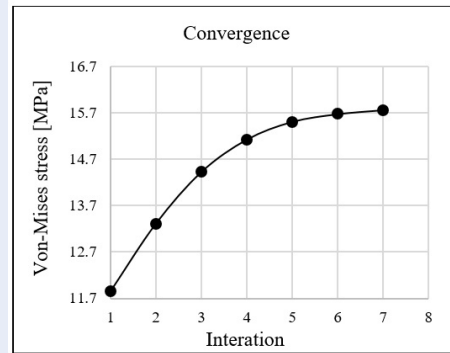


Figure 10: Convergence Diagram for 40% Trimline

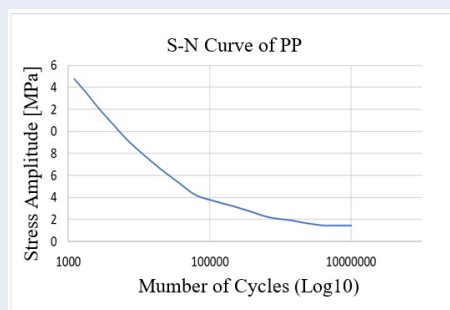


Figure 11: S-N Curve of Polypropylene

show that for a thickness of 2 mm, the fatigue life is very low, if considering the life in days, on the 8th day, then the fatigue failure begins to occur, and thus the 2 mm thickness is considered to fail to meet fatigue standards. For the 3 mm thickness model, it seems that the destruction will start from the 680th day after 524850 steps. Therefore, it is found that this AFO has a durability of about 2 years and 3 months. A factor of safety less than 1 indicates that the AFO will fail before its design life is reached.

Through this fatigue analysis, it can be concluded that a thickness of 3 mm should be applied, but for safety reasons, after using from 1 and a half to 2 years, the AFO should be replaced. The 4mm model, despite its high fatigue strength, but so thick that the AFO becomes significantly heavier by about 30% compared to 3mm.

CONCLUSION AND OUTLOOK

The bending moment results in this study allowed clinicians to estimate the stiffness required for the AFO, and then the required trimline could be determined. There are several limitations in this study that should be noted. Firstly, only one patient AFO was used, which excludes the impact of the patient's foot

size and shape on AFO behavior. In addition, the simulation with the assumed constraints does not resemble the practical model. Although this may not fully represent the motions of the AFO under walking conditions, it does give a reasonable and approximate value for the stiffness to which the AFO is subjected. A preliminary analysis was performed to estimate the life of the AFO under the stated conditions. One surprise was that the predicted life to failure varied greatly with AFOs of different thicknesses. AFO with a thickness of 3 mm is highly recommended to ensure its life expectancy in a long run. Nonetheless, it is noticeable that AFOs with a thickness above 3mm may cause discomfort when used.

ACKNOWLEDGMENT

This research is funded by the Ho Chi Minh City University of Technology – VNU-HCM, under grant number SVCQ-2020-KHUD-42. In addition, we acknowledge the support of time and facilities from Ho Chi Minh City University of Technology (HCMUT), VNU-HCM, for this study.

NOMENCLATURES

AFO: Ankle Foot Orthosis
 FEM: Finite Element Method
 PP: Polypropylene

CONFLICT OF INTEREST

The Group of authors declares that this manuscript is original, has not been published before, and there is no conflict of interest in publishing the paper.

AUTHOR CONTRIBUTION

Thien Tich Truong is the supervisor, contributes ideas for the proposed method checking the numerical results.

Khuong Nguyen Trieu is working as the chief developer of the method and the manuscript editor.

REFERENCES

- Halar E, Cardenas DD. Ankle-foot orthoses: clinical implications. *Physical Medicine and Rehabilitation*. 1987;1(1):45-66.
- Liu Z, et al. The Application Study of Specific Ankle-Foot Orthoses for Stroke Patients by 3D Printing Somos Next. *Journal of Biomaterials and Tissue Engineering*. 2019;9(6):745-750; Available from: <https://www.ingentaconnect.com/contentone/asp/jbte/2019/0>.
- Lovegreen W, Pai AB. Orthoses for the Muscle Disease Patient. *Atlas of Orthoses and Assistive Devices*, Elsevier. 2019;332-336; Available from: <https://www.sciencedirect.com/science/article/pii/B978032348320000329?via%3Dihub>.
- Skaaret I, et al. Comparison of gait with and without ankle-foot orthoses after lower limb surgery in children with unilateral cerebral palsy. *Journal of Children's Orthopaedics*. 2019;13(2):180-189; Available from: <https://pubmed.ncbi.nlm.nih.gov/30996743/>.

5. Arnold MA. Finite element analysis of ankle foot orthoses. PhD Thesis, University of Southampton, 1999;
6. Golay, et al. The effect of malleolar prominence on polypropylene AFO rigidity and buckling. *Journal of Prosthetics and Orthotics*. 1989;1(4):231-241; Available from: https://journals.lww.com/jpojournal/Citation/1989/07000/The_Effect_of_Malleolar_Prominence_on.7.aspx.
7. Yamamoto S, et al. Comparative study of mechanical characteristics of plastic AFOs. *Journal of Prosthetics and Orthotics*. 1993;5(2):59-64; Available from: <https://doi.org/10.1097/00008526-199304000-00009>.
8. Lord M, Jones D. Issues and themes in computer aided design for external prosthetics and orthotics. *J. Biomed. Engng*. 1988;10(6): 491-498; Available from: [https://doi.org/10.1016/0141-5425\(88\)90106-9](https://doi.org/10.1016/0141-5425(88)90106-9).
9. Darwich A, et al. Ankle-foot orthosis design between the tradition and the computerized perspectives. *The International Journal of Artificial Organs*. 2019; 43(5):354-361; Available from: <https://doi.org/10.1177/0391398819890348>.
10. Leone D, et al. Structural stability prediction for thermo-plastic ankle-foot orthoses. In *Proceedings of the 17th Annual Northeast Bioengineering Conference*, Hartford, Connecticut. 1991 Apr;231-232; Available from: <https://doi.org/10.1109/NEBC.1991.154659>.
11. Chu TM, et al. Three dimensional finite element stress analysis of the polypropylene, ankle-foot orthosis: static analysis. *Med. Engng Physics*. 1995;17(5):372-379; Available from: [https://doi.org/10.1016/1350-4533\(95\)97317-1](https://doi.org/10.1016/1350-4533(95)97317-1).
12. Shear AB, et al. Trimline Severity Significantly Affects Rotational Stiffness of Ankle-Foot Orthosis. *Journal of Prosthetics and Orthotics*. 2010; 22(4):204-210; Available from: <https://doi.org/10.1097/JPO.0b013e3181f9082e>.
13. Surmen HK, et al. Evaluation of various design concepts in passive ankle-foot orthoses using finite element analysis. *Engineering Science and Technology, an International Journal*. 2021;24(6):1301-1307; Available from: <https://doi.org/10.1016/j.jestch.2021.03.004>.
14. Condie DN, Meadows CB. Some biomechanical considerations in the design of ankle-foot orthoses. *Orthotics and Prosthetics*. 1977;31(3):45-52; Available from: http://www.oandplibrary.org/op/1977_03_045.asp.
15. ; Available from: http://mms2.mines-paristech.fr/msi_paris/nlfe/transparents/paris_tech2005a.pdf.
16. ; Available from: https://royomech.org/Useful_Tables/Fatigue/Stress_levels.html.
17. Lehmann JF, et al. Plastic ankle-foot orthoses: evaluation of function. *Arch. Phy. Med. Rehabil*. 1983;64(9):402-407; Available from: <https://pubmed.ncbi.nlm.nih.gov/6615177/>.
18. ; Available from: <https://omnexus.specialchem.com/selection-guide/polypropylene-pp-plastic>.
19. Sumiya T, et al. Stiffness Control in Posterior-type Plastic Ankle-foot Orthoses: Effect of Ankle Trimline. *National Library of Medicine*. 1996;20(2):129-131; Available from: <https://doi.org/10.3109/03093649609164431>.
20. Yasuhiro M, Takamichi T, et al. An Evaluation Technique of the Fatigue Analysis of an Ankle-Foot-Orthosis in the Design Process. 2008 Apr;4(74):884-889; Available from: <https://doi.org/10.1299/kikaic.74.884>.